Article

Microstructure Evaluation of Fly Ash Geopolymers Alkali-Activated by Binary Composite Activators

JiangPing Zhao [1] and YaChao Wang [1,*]

[1] School of Resources Engineering, Xi'an University of Architecture & Technology, Xi'an, 710055, China
* Correspondence: wangyachao@xauat.edu.cn

Abstract: An attempt to investigate the effect of binary composite activators on the microstructure of fly ash-based geopolymers is conducted through the comparison of 24 experiments, which consisted of $Na_2SiO_3 \bullet 9H_2O$, Na_2CO_3, K_2CO_3, NaOH, and KOH through a facile preparation technique. The results show that the activator of $Na_2SiO_3 \bullet 9H_2O$+KOH presents the highest mechanical strength, due to the synergy activation between the inherent ≡Si-O-Si≡ chains derived from Na_2SiO_3 and K^+'s catalysis. It reveals that the K^+ plays a crucial role in Na_2SiO_3-activated fly ash geopolymer, which is the rate-determining step of the enhanced crosslinking and propagation of N-(C)-A-S-H chains, leading to an increase in weight loss temperatures of specimens from TG/DTG results. Furthermore, the adding silica fume facilitates as-formed amorphous silicates, which also could fill into the pores of N-(C)-A-S-H amorphous gels and present a uniform and compact morphology, leading to an increase in the pore volume of the pore diameter less than 100 nm. It explores an efficient and cost-effective preparation of fly ash-based geopolymer for developing solid-waste recycling techniques.

Keywords: Alkali-activated; Microstructure; Fly ash; Binary activator; Crosslinking

1. Introduction

The mechanisms governing the formation of alkali-activated fly ash-based geopolymer have been an area of intense investigation [1-2], as an alternative to traditional Portland cement, one of the fundamental assumptions in the study of geopolymer formation has been that soluble alumina and silica that undergo a dissolution–reorientation–solidification process to form geopolymeric materials, further studies are still critical for its pervasive application [3-5]. According to the reports of journal literature on fly ash-based geopolymer [6-7], phosphoric acid and alkaline activators such as Na_2SiO_3, NaOH, K_2SiO_3, and KOH, could make the reactive silicates and aluminates in fly ash depolymerize and restructure into N-(C)-A-S-H amorphous gels, which serves as cementitious material to replace the ordinary cement. Generally, an efficient and cost-effective fabrication of fly ash-based geopolymer is urgent and necessary to develop solid-waste recycling techniques

Currently, the exploration and research on the binary composite activators have been important issues, to obtain excellent usability and low preparation cost. Komljenovic[8] used aqueous solutions of $Ca(OH)_2$, NaOH, NaOH+Na_2CO_3, KOH, and sodium silicate (water glass) of various concentrations as alkali-activators, proposed that the high strength was directly related to the high Si/Al ratio; the greater the Si/Al ratio in the reaction products, the higher the strength. And the activation potential of the activators investigated (taking equal concentrations into account) could be represented by the following: KOH < NaOH + Na_2CO_3< NaOH < $Na_2O \cdot nSiO_2$. Cheng [9] found that with increasing K_2O content, the setting time increased, the compressive strength raised, and the fire resistance characteristics were also improved in slag-based geopolymers. It was found that calcium ions did not simply balance the charge, but also acted as structural links to maintain the connectivity of the geopolymer network and induced a more condensed structure as long poly-sialate chains suggesting high cross-linking geopolymerical frameworks [10]. The $Ca(OH)_2$ mixing with K_2CO_3 as an alkaline activator solution was used to prepare a kaolin-based geopolymer[11]. Wang et al.[12] investigated the effect of alkali admixture, activator modulus, and water–binder ratio on the workability,

Preprints (www.preprints.org) | NOT PEER-REVIEWED | Posted: 2 June 2023 doi:10.20944/preprints202306.0148.v1

rheology, and geopolymerization of fly ash geopolymer activated by the composite of sodium hydroxide and sodium silicate. Similarly, the carbonate and potassium have been explored for geopolymerical preparation, but there is fewer literature to conduct a comparative study on the micro-structures of fly ash-based geopolymer activated by the single KOH, NaOH, Na_2CO_3, K_2CO_3, Na_2SiO_3 and their binary composites.

Furthermore, the composite activators consisting of solid waste have been intriguing the increasing attention, such as calcium carbide residue and Glauber's salt [13], calcium carbide slag and sodium metasilicate powder [14], salt-loss soda residue and oxalate acid [15]. Essentially, the alkali-activation is the interactions between the cations like K^+, Na^+, and Ca^{2+} and anions like CO_3^{2-}, OH^-, SiO_3^{2-}, and PO_4^{3-}, which could facilitate or inhibit the crosslinking or grafting reactions among the N-(C)-A-S-H chains involved in the geopolymers. The as-formed robust and cross-linked network structures exert excellent mechanical strength and duration in theory.

However, regarding the fly ash-based geopolymer, previous research has failed to consider the synergy between K^+ and SiO_3^{2-}, on the way to deepening the geopolymerical mechanisms. It preliminarily focuses on the synergetic effects of cations like K^+, Na^+, and anions like CO_3^{2-}, OH^-, SiO_3^{2-} in this article. A series of comparative studies on the micro-structures and mechanical performance of fly ash-based geopolymer is conducted systematically, which is activated by various alkaline binary activators with different concentrations including $Na_2SiO_3 \bullet 9H_2O$, Na_2CO_3, K_2CO_3, NaOH, and KOH, respectively. The techniques are employed to clarify the micro-structure of different samples, including the testing of mechanical strength, scanning electron microscope (SEM), mercury intrusion porosimetry (MIP), thermogravimetry/differential thermogravimetry (TG/DTG), and X-ray diffraction (XRD). It determines the optimum formulation of the alkaline binary composite activator for preparing the fly ash-based geopolymer, elucidating the corresponding mechanism among the various binary activators to prepare the geopolymer with effective-cost performance.

2. Materials and characterization

2.1. Starting materials and preparation of specimens

Fly ash was obtained from the Hancheng power plant and ground to the Blaine specific surface area of 560 m^2/kg with a density of 2.45 g/cm^3, its average particle diameter equaled 11.8 μm tested by a laser particle size analyzer, and the chemical composition was measured by X-ray fluorescence (XRF) as shown in Table 1. Alkali-activators, including $Na_2SiO_3 \bullet 9H_2O$, Na_2CO_3, K_2CO_3, NaOH, and KOH, were purchased from Xi'an chemical reagent company, they belonged to the grade of analytical reagent chemical.

Table 1. Chemical composition of fly ash (wt%).

Composition	SiO_2	Al_2O_3	Fe_2O_3	CaO	K_2O	SO_3	TiO_2	Loss
Weight percent	50.16	36.25	4.46	3.85	1.84	0.54	1.18	1.76

2.2. Preparation of specimens

The $Na_2SiO_3 \bullet 9H_2O$ (15wt%), Na_2CO_3 (1mol/L, 2mol/L), K_2CO_3 (1mol/L, 2mol/L), NaOH (4mol/L, 8mol/L), KOH (4mol/L, 8mol/L) and their binary composite solutions were employed as alkali-activator as shown in Table 2, respectively. The fly ash-based geopolymerical specimens were prepared by stirring a mixture of fly ash and activator solution with a water/FA ratio of 0.30 to form the slurry in the cement mortar machine of SJ-160 type and then poured the slurry into the stainless triplet mold of $50 \times 32.5 \times 32.5 mm^3$ with 1 minute vibrating on the vibrating table of ZT-96 type, demoulded after curing for 9h at an elevated temperature of 85°C in the oven, finally specimens were cured for another 27 days in curing chamber at room temperature with a 90% humidity to evaluate their performances.

To understand the effects of different ions during the process of geopolymerization further, silica fume (SF) as a supplier of activated Si units was applied to preparing the specimen by mixing 10 wt% SF with 90 wt% fly ash as starting materials. The S25~S27 corresponds to the samples of fly ash/SF

Preprints (www.preprints.org) | NOT PEER-REVIEWED | Posted: 2 June 2023 doi:10.20944/preprints202306.0148.v1

(fly ash: SF=90:10, wt%) geopolymer, which was activated by 15% Na_2SiO_3, 15%Na_2SiO_3+4M KOH, and 15% Na_2SiO_3+2M K_2CO_3, respectively.

2.3. Characterizations

Compressive strengths were tested by a full-automatic cement compressive testing machine of YAW-300 type with a pressurization rate of 2.4 kN/s. Morphology analysis was conducted on a Quanta 200 scanning electron microscope (SEM) with a working voltage of 20kV and a vacuum degree of 10^{-5} torr. Thermogravimetric analysis (TGA) of Mettler measured the real-time weight loss of specimens during the heating process of 50-950℃ under a nitrogen atmosphere at a heating rate of 30℃/min. Pore size distributions of samples were measured by AUTOPORE 9500 mercury intrusion porosimetry (MIP) under a nitrogen pressure of 0.3 MPa. X-ray diffraction (XRD) patterns of specimens were measured on a D/MAX-2400 X-ray diffractometer equipped with a rotation anode using Cu Kα radiation.

3. Results

3.1. Mechanical properties

The compressive strengths of specimens with different alkali activators are shown in Table 2. It is noted that all specimens exhibit an increase in the compressive strength from the aging of 3d to 28d, respectively, indicating the geopolymerization involved in various systems has not completely reacted after heat curing of 85℃ for 9h. The single k^+-based activators exhibit weaker activation efficiency than Na^+, considering the strength as the reference.

The highest compressive strength presents on specimen S17 with binary composite activators of 15wt% $Na_2SiO_3{\cdot}9H_2O$+4mol/L KOH, it gets 56.08MPa at an aging of 28d. It is in agreement with the Juho that the use of potassium silicate rather than sodium aluminate as an activator result in higher strength [16]. However, the excess NaOH is harmful to the mechanical strength, leading to a decrease in the compressive strength. Gökhan[17] found that the optimal thermal curing temperature and the optimal NaOH concentration were 85°C and 6 M, respectively.

Assuming using the compressive strength as an evaluation criterion of the activation efficiency, it is directly related to mechanical strength, it can be identified as the following (taking into account the equal concentration of cations): (1) as for the K^+, K_2CO_3<K_2CO_3+KOH<KOH, (2) as for the Na^+, Na_2CO_3<Na_2CO_3+KOH<Na_2CO_3+NaOH<NaOH, (3) as for the binary mixture, Na_2SiO_3+NaOH<Na_2SiO_3+Na_2CO_3<Na_2SiO_3+K_2CO_3<Na_2SiO_3+KOH, respectively.

Table 2. Compressive strength of specimens with different alkali-activators.

Sample	Activator composition					Compressive strength (MPa)		
	$Na_2SiO_3{\cdot}9H_2O$	Na_2CO_3	K_2CO_3	NaOH	KOH	3d	7d	28d
S1	15wt%	0	0	0	0	19.83	20.08	20.25
S2	0	1mol/L	0	0	0	1.50	1.58	1.75
S3	0	2mol/L	0	0	0	2.00	2.42	5.25
S4	0	0	1mol/L	0	0	0.08	0.17	0.17
S5	0	0	2mol/L	0	0	0.17	0.17	0.25
S6	0	0	0	4mol/L	0	4.83	5.25	6.42
S7	0	0	0	8mol/L	0	21.33	23.00	15.67
S8	0	0	0	0	4mol/L	2.08	2.17	2.30
S9	0	0	0	0	8mol/L	15.92	11.83	10.80
S10	0	0	0	4mol/L	4mol/L	8.75	10.83	9.58
S11	0	0	0	8mol/L	4mol/L	21.83	33.25	30.92
S12	15wt%	1mol/L	0	0	0	29.10	31.25	32.50
S13	15wt%	2mol/L	0	0	0	30.67	33.08	35.50
S14	15wt%	0	1mol/L	0	0	33.67	34.82	39.17
S15	15wt%	0	2mol/L	0	0	38.08	40.25	43.08
S16	15wt%	0	0	4mol/L	0	**9.63**	10.42	10.67
S17	15wt%	0	0	0	4mol/L	**54.08**	54.67	56.08

Preprints (www.preprints.org) | NOT PEER-REVIEWED | Posted: 2 June 2023 doi:10.20944/preprints202306.0148.v1

S18	15wt%	0	0	0	8mol/L	**51.71**	53.93	55.17
S19	0	1mol/L	0	4mol/L	0	17.50	17.92	18.25
S20	0	2mol/L	0	4mol/L	0	20.17	21.08	21.92
S21	0	0	1mol/L	0	4mol/L	4.92	4.92	5.17
S22	0	0	2mol/L	0	4mol/L	4.25	4.50	4.68
S23	0	2mol/L	2mol/L	0	0	0.17	0.17	0.25
S24	0	2mol/L	0	0	4mol/L	5.25	5.42	5.50

However, excess OH^- holds an adverse effect, to the disadvantage of the compressive strength, the strength (10.67 MPa) of specimen S16 with Na_2SiO_3+NaOH activated is inferior to the specimen (S1, 20.25 MPa) with Na_2SiO_3 activated only, it is in agreement with the report of Kiatsuda et al.[18] that a critical OH^- is crucial to attaining a specimen with excellent mechanical performance. And Chindaprasirt et al.[19] suggest the NaOH concentration affects the ettringite formation and lowers the strength. However, the single K-activators including KOH and K_2CO_3 exert the lower activation, while the K^+ altogether with Na_2SiO_3 exhibits the highest activation efficiency. It induces that the K^+ altogether with $Si(OH)_4$ is beneficial for obtaining a higher mechanical strength of fly ash-based geopolymer, the detailed reasons are illustrated in the section of the discussion.

Interestingly, incorporating the 10 wt% SF triggers an obvious enhancement of the mechanical strength as shown in Fig.1, that of the specimen activated by the mixture of $Na_2SiO_3{\cdot}9H_2O$ and KOH rises to 83.58 MPa (increased by 49%). It means that the activated ≡Si-O-Si≡ chains play a fundamental role in forming a crosslinked network structure, but K^+ presents a rate-determining factor for improving strength further.

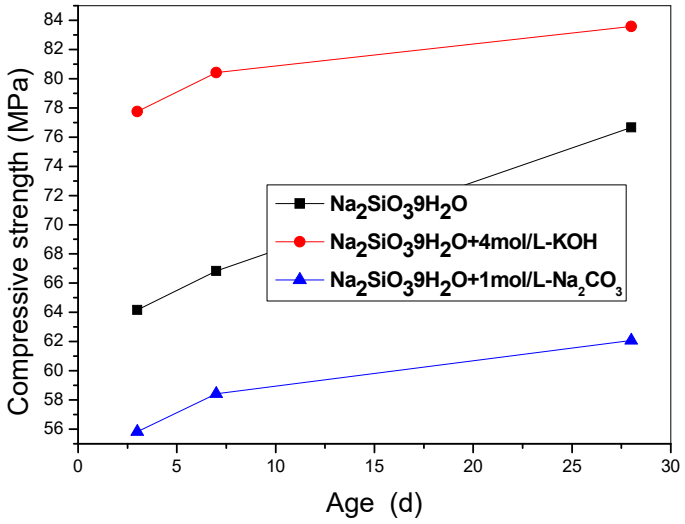

Figure 1. The compressive strength of specimens incorporated SF including S25~S27.

3.2. Morphology and Microstructure

Morphologies of specimen pastes at 28d aging are displayed as a series of SEM images with a magnification of 5000 in Fig.2a-h, unreacted spherical FA particles decrease and transform into irregularly shaped gels on the fracture surface of pastes, displaying the coexistence of the geopolymeric gels and partially activated FA particles. It is observed that the activation efficiency of single NaOH is superior to KOH compared the Fig.2a with Fig.2b, more amorphous gels present on the fracture surface of NaOH-activated paste.

However, it is worth pointing out that the Na^+ involved in the alkali-activator is prone to forming porous and unevenly distributed framework structures shown in Fig.2c, Fig.2f, and Fig.2h, respectively. While activators with K^+ facilitate the formation of plate-type or rod-like structures as shown in Fig.2d, Fig.2e, and Fig.2g, respectively. Especially for the uniform and smooth fracture in Fig.2e, corresponding to the enhanced strength. It indicates that the K^+ favors the condensations or

Preprints (www.preprints.org) | NOT PEER-REVIEWED | Posted: 2 June 2023 doi:10.20944/preprints202306.0148.v1

crosslinking between SiO_4^{4-} and AlO_4^{5-} tetrahedra and boosts the chain propagation of N-(C)-A-S-H amorphous gels, evidenced by the improved compressive strength. Meanwhile, the porosity of the Na-specimen seems to be multiscale in Fig.2f and Fig.2h, this feature is less pronounced for K-specimen as shown in Fig.2e and Fig.2g, it is in agreement with the Prudhomme [20].

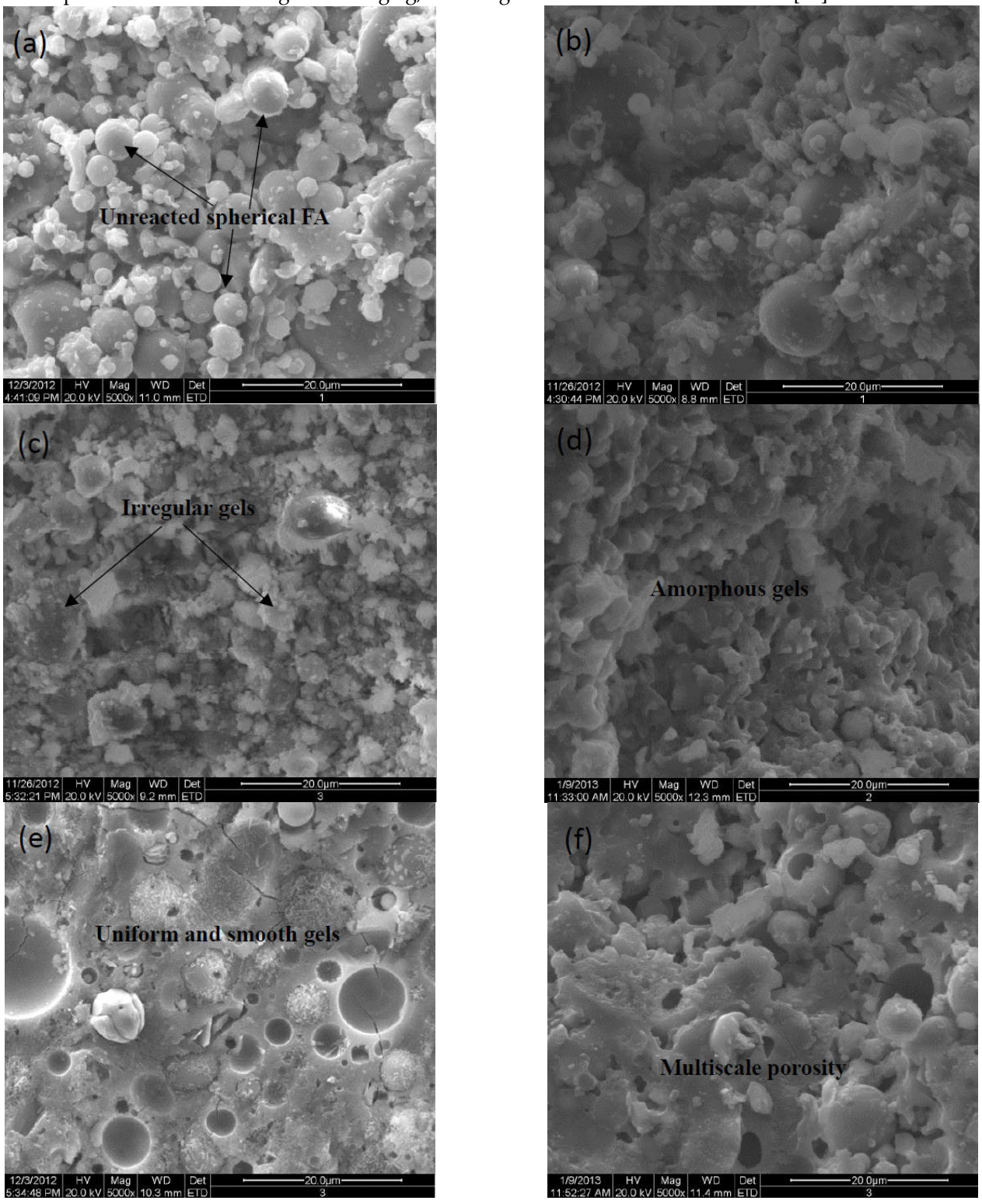

Preprints (www.preprints.org) | NOT PEER-REVIEWED | Posted: 2 June 2023 doi:10.20944/preprints202306.0148.v1

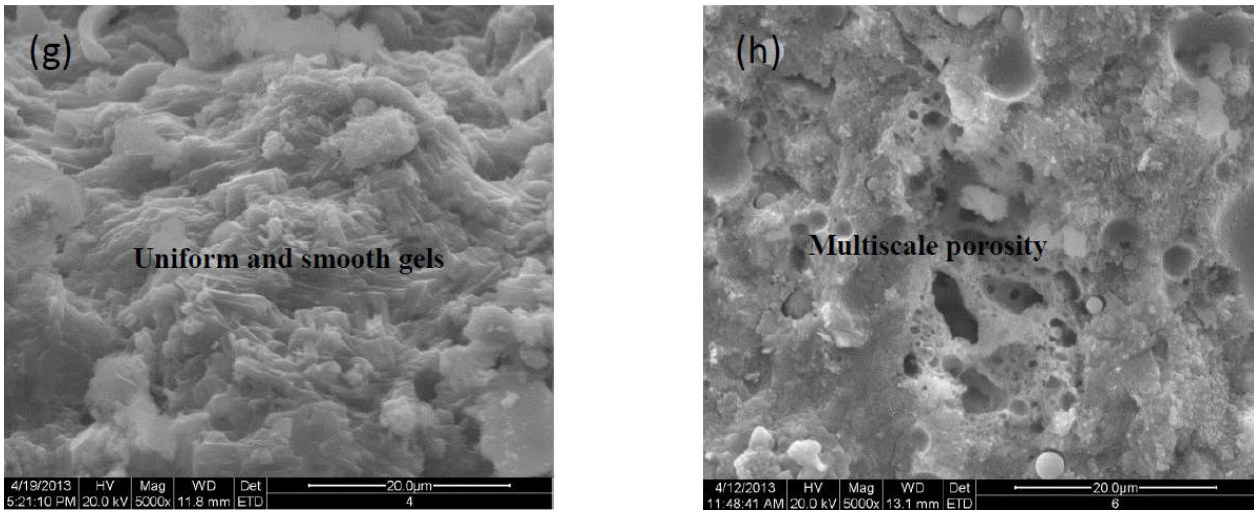

Figure 2. SEM photos of samples with a magnification of 5000× (a) 4mol/L-KOH, (b) 4mol/L-NaOH, (c)15wt%Na_2SiO_3, (d) 4mol/L -KOH+8mol/L-NaOH, (e) 15wt%Na_2SiO_3+4mol/L-KOH, (f) 15wt%Na_2SiO_3+4mol/L-NaOH, (g) 15wt%Na_2SiO_3+1mol/L-K_2CO_3, (h) 15wt%Na_2SiO_3+ 1mol/L-Na_2CO_3.

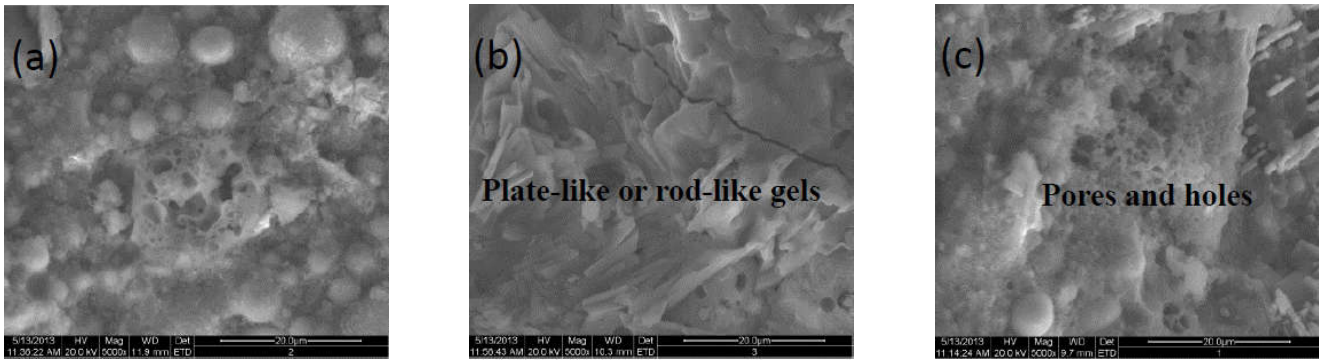

Figure 3. SEM photos of geopolymer incorporated 10wt% SF with a 5000×. (a) 15wt%Na_2SiO_3, (b) 15wt%Na_2SiO_3+4mol/L-KOH, (c) 15wt%Na_2SiO_3+1mol/L-Na_2CO_3.

To further understand the details of micro-appearance, morphologies of specimens incorporated 10 wt% SF at 28d aging are displayed in Fig.3, the plate-like or rod-like structures appear on the fracture surface of the specimen with the composite activator of 15wt% $Na_2SiO_3 \cdot 9H_2O$ and 4mol/L KOH in comparison to others, while more pores and holes present on the fracture surface as in Fig.3a and Fig.3c. It confirms again that the K^+ boosts the densification process significantly in Na_2SiO_3 activated fly ash-based geopolymer.

For the sake of exploring the microstructures involved in the specimens with K^+, the pore size distribution of specimens is summarized in Table 3, it is noted that adding KOH in the composite activators makes the median pore diameter and porosity decline in comparison to the S1. Because the pore volume with a pore diameter less than 100 nm increases while that with a pore diameter more than 0.2 μm decreases, matching the enhanced mechanical properties. Because the composite activator (15wt%Na_2SiO_3+4mol/L-KOH) facilitates more silicate depolymerization and transforms into siliceous sols, which favors the binder's densification. Especially for the SF-containing samples, the median pore diameter further decreases to 67.1 nm from 74.6 nm, because of the pozzolanic effect and filling of SF. Generally, the pore size distribution also provides indirect evidence for the highest activation efficiency of 15wt%Na_2SiO_3+4mol/L-KOH.

Preprints (www.preprints.org) | NOT PEER-REVIEWED | Posted: 2 June 2023 doi:10.20944/preprints202306.0148.v1

Table 3. Pore size distribution of specimens.

Specimens	<100nm（%）	100-200nm（%）	>0.2μm（%）	Median pore diameter (nm)	Porosity（%）	Total intrusion volume（ml/g）
S1	0.56	14.53	84.91	239.7	23.98	0.1961
S15	27.87	14.18	57.95	104.8	21.36	0.1719
S17	52.54	2.16	45.31	74.6	19.69	0.1578
S25	53.67	6.94	39.39	67.1	19.52	0.1523

S25, the specimen with 10 wt% SF and activated by 15wt%Na_2SiO_3+4mol/L-KOH

3.3. TG/DTG analysis

The TGA/DTG results of specimens are illustrated in Fig.4. The weight loss and DTG peak temperature of specimen S1 activated only by 15wt% Na_2SiO_3 are 6.05%, 76.3°C and 123.5°C respectively, that of specimen S15 with 15wt%Na_2SiO_3+2mol/L-K_2CO_3 activated is 10.06%, 98.6 and 178.1°C, that of specimen S13 activated by 15wt%Na_2SiO_3+2mol/L-Na_2CO_3 is 10.28%, 92.8 and 175.8°C, that of specimen S17 activated by 15wt%Na_2SiO_3+4mol/L KOH is 8.91%, 71.1 and 182.8°C, that of specimen S16 activated by 15wt%Na_2SiO_3+4mol/L NaOH is 4.51%, 71.5 and 149.7°C, respectively. The first peak temperature below 100 °C corresponds to the maximum weight loss, is mainly attributed to the free water loss within the geopolymer. While the second peak is mainly attributed to the dehydration of chemical-bonded water within the N-(C)-A-S-H amorphous gels. The S17 exhibits the highest temperature of the second peak, due to the compact and denser structure.

The weight loss mainly derives from the occurrence of dehydration involved in specimens below 300°C, dehydroxylation derived from $Si(OH)_4$ or $[Al(OH)_4]^-$ tetrahedron occurs at about 500°C[21], more weight loss implies more hydroxyls exist within matrix during the process of alkali-activation. Combined with the results of pore size distribution, it could be induced that the more volume of small pores, the higher temperature of weight loss. The DTG curves of K-specimens display twists and turns as shown in Fig.4(b) and Fig.4(d), meaning more complex and crosslinking structures involved in the specimens compared to the curves of others. It indirectly demonstrates that doping K^+ promotes the formation of the amorphous and more net-work cross-linking of Na_2SiO_3 activated fly-ash based geopolymer.

Preprints (www.preprints.org) | NOT PEER-REVIEWED | Posted: 2 June 2023 doi:10.20944/preprints202306.0148.v1

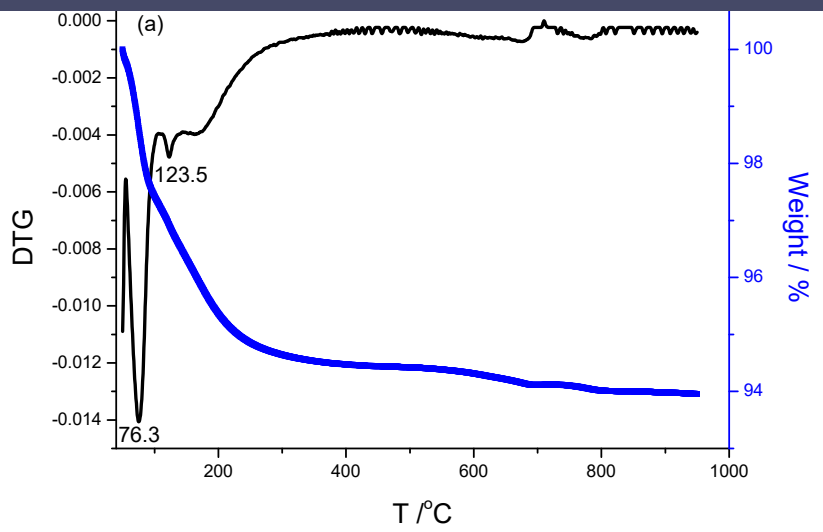

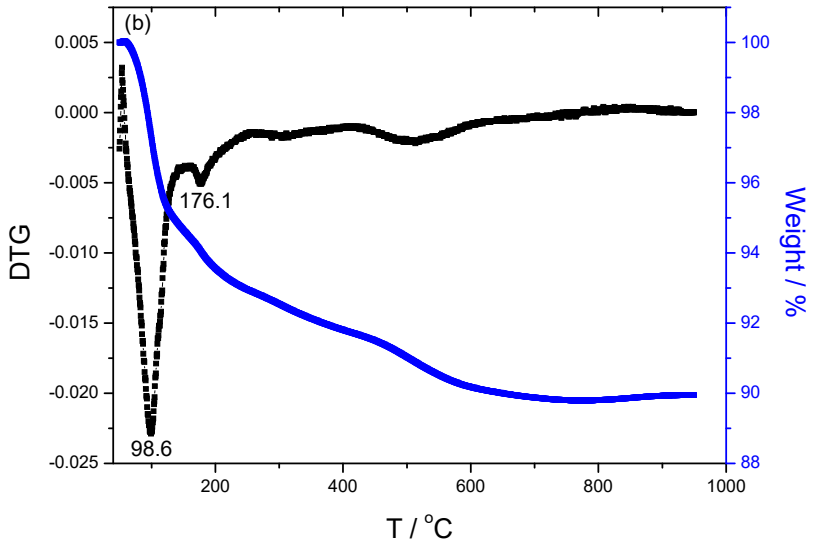

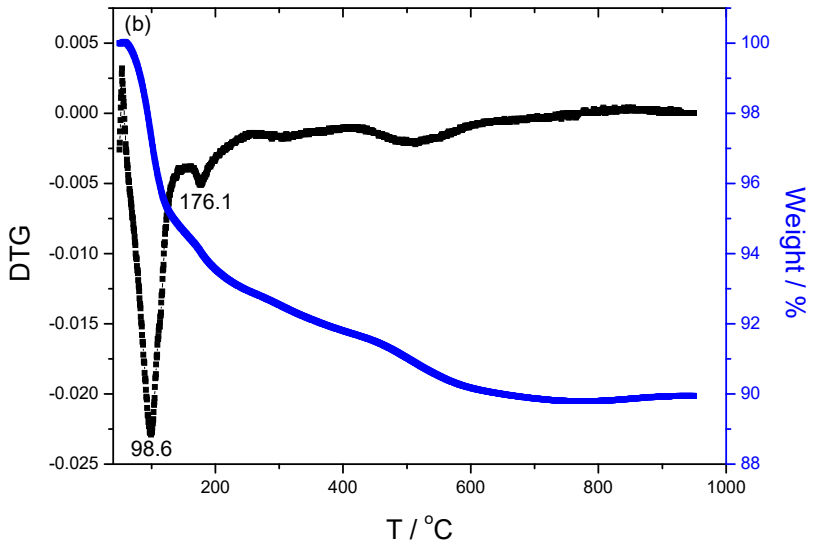

Preprints (www.preprints.org) | NOT PEER-REVIEWED | Posted: 2 June 2023 doi:10.20944/preprints202306.0148.v1

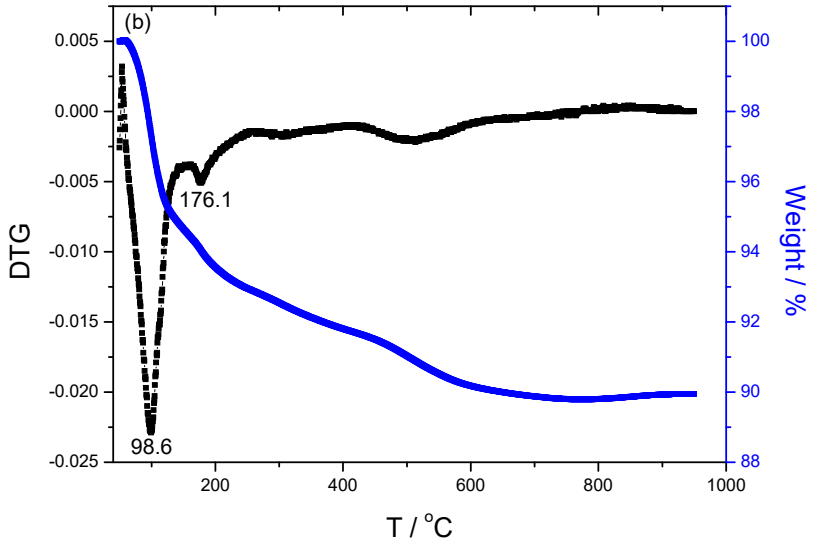

Figure 4. Thermogravimetric analysis of samples including (a)S1 activated by 15wt%Na_2SiO_3, (b) S15 activated by 15wt%Na_2SiO_3+2mol/L-K_2CO_3, (c) S13 activated by 15wt%Na_2SiO_3+2mol/L-Na_2CO_3, (d) S17 activated by 15wt%Na_2SiO_3+4mol/L-KOH, and (e) S16 activated by 15wt%Na_2SiO_3+4mol/L-NaOH, respectively.

3.4. XRD analysis

There are some peaks derived from the raw fly ash, such as the quartz, mullite, and silimanite, but the peaks at about 2θ=27.5, 29.5, 32.3, 24.9 are assigned to the orthoclase [22], as shown in Fig.5. The broad and diffused peaks of about 2θ=30 are the results of the short-range glassy structures [23]. It is obvious that the area between the patterns and the baseline increases after adding SF into the system (Area 2> Area 1), due to the increased amorphous silicates. The orthoclase grows and develops with the increasing content of amorphous $Si(OH)_4$, it is in agreement with that increasing the Si/Al ratio in the gels causes the formation of more silicon-rich mineral phases, as orthoclase and sanidine ($K[AlSi_3O_8]$) [24].

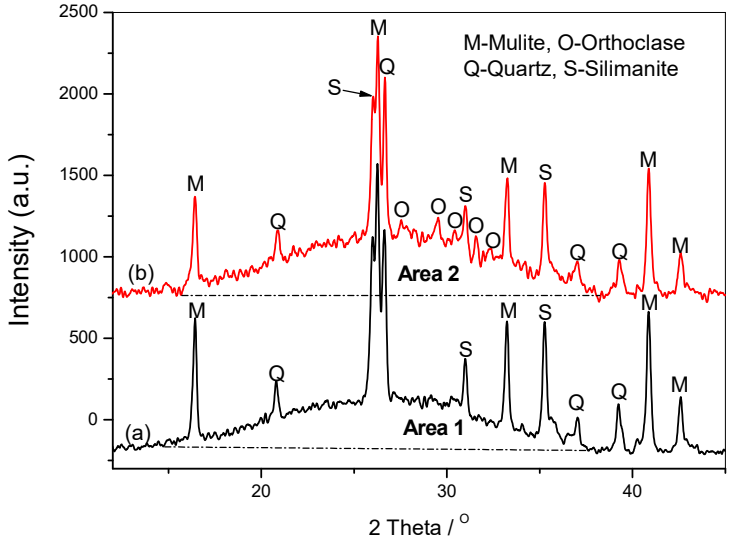

Figure 5. The XRD spectra of samples S17 activated by15wt%Na_2SiO_3+4mol/L-KOH including (a)sample without SF, (b) SF-containing sample.

Preprints (www.preprints.org) | NOT PEER-REVIEWED | Posted: 2 June 2023 doi:10.20944/preprints202306.0148.v1

4. Discussion

Generally, the mechanical strength and microstructure of fly ash geopolymers alkali-activated by binary composite activators are comparatively studied, and the alkaline activators are composed of $Na_2SiO_3 \bullet 9H_2O$, Na_2CO_3, K_2CO_3, NaOH, and KOH. The composite activator of $Na_2SiO_3 \bullet 9H_2O$+KOH exerts the highest activation efficiency evidenced by the enhanced strength and reduced porosity, due to the enhanced crosslinking and propagation of N-(C)-A-S-H chains, leading to the increased content of the amorphous silicates with uniform and compact morphology, as well as the improved temperature of DTG peak.

Because Na holds a higher charge density and smaller ionic radius than K, thus the OH^- has higher accessibility to Si-O and Al-O bonds in the Na-rich surfaces than K-rich surfaces [25], the ionic radii proposed for five- and six-coordinate sodium are 1.02 and 1.07 Å, respectively, while the ionic radii for six- and seven-coordinate K^+ are 1.38 and 1.46 Å, respectively [26]. Essentially, potassium has a smaller hydration sphere than sodium, which is a small alkaline element. Therefore, potassium has a weaker affinity to water than sodium [27]. It explains the inferior activation efficiency of the single KOH solution to pure NaOH solution. Because the reactive N-(C)-A-S-H is too little to trigger crosslinking, instead the high OH- inhibits or interrupts the chain propagation.

However, the composite activator including K^+ and SiO_3^{2-} is crucial to trigger more geopolymerization and forming more amorphous networks. The doped Na_2SiO_3 holds the inherent chain structure ≡Si-O-Si≡, which severs as the "condensation nucleus" to facilitate the further crosslinking and propagation of N-(C)-A-S-H chains. A similar phenomenon also pronounces in SF-based geopolymer, K^+ together with Na_2SiO_3 is beneficial for the formation and growth of siliceous gels beneficial for the formation and growth of siliceous gels [27]. The mixture solution of KOH and Na_2SiO_3 presents a superior performance than that of NaOH and Na_2SiO_3, and the composite activator with 4 M KOH is better than that of 8 M KOH. Because the excessive alkalinity makes more ions dissolve and precipitate [28], which restrains some alkali metal ions to participate in the propagation of N-(C)-A-S-H chains, and the K^+ concentration in the medium is not as pH-dependent as Na^+ [29].

Secondly, water and potassium transform into interconnected networks through hydrogen bonding, the K^+-H_2O hydrogen-bonded network holds a stabilizing effect [24]. While the Na^+ could not convert into the hydrogen-bonded networks. It means more widespread K^+ exists in the system, providing the sustained catalysis for the polycondensations among N-(C)-A-S-H chains, due to the K^+ contributing a higher disorder degree or crosslinking for the K-based system [30]. Furthermore, Cioffi et al. [31] also suggest that the larger size of potassium has a favorable effect on cross-linking even if the polycondensation degree left is unchanged, which is beneficial for the distortion, transformation, and cross-linking, leading to an increased endothermic peak and denser morphology.

Thirdly, due to the lower viscosity of KOH solution in comparison with NaOH [32], it also plays a critical role in geoploymerications involved in the system containing sufficient activated $Si(OH)_4$, leading to enhanced mechanical strength, while higher NaOH concentration solution causes aluminosilicate gels precipitation at a very early stage.

Furthermore, the SF-containing specimen also proves this point. The increased activated $Si(OH)_4$ provides the beneficial conditions for K^+ to form more cross-linked N-(C)-A-S-H chains, leading to an obvious increase in strength. Our finding confirms that the K^+ predominantly controls the step of reorganization in fly ash-based geopolymerical system, according to the process of "depolymerization-reorganization". The evolution process of K^+ in the alkali-activated fly ash system is affected not only by the activator (e.g., composition) but also by the concentration (e.g., 4 M and 8 M).

Consequently, the depolymerizations of silicates occur and form some $Si(OH)_4$ and $[Al(OH)_4]^-$ monomers under stronger alkali-condition, but the in-situ crosslinked ≡Si-O-Si≡ chains as the"condensation nucleus" provide the preconditions of the subsequent polycondensations or propagation of N-(C)-A-S-H. The K^+ in the composite activators boosts the reorganization or restructuring of activated alumina and silica, the as-formed amorphous sols could fill into the pores and holes corresponding to enhanced strength, leading to an increase in the pore volume of the

 doi:10.20944/preprints202306.0148.v1

diameter less than 100 nm, as well as an increase in weight loss temperatures of specimens from TG/DTG results.

5. Conclusions

The comparative study on the microstructure of fly ash-based geopolymer activated by binary composite activator is investigated by characterization techniques, which consists of $Na_2SiO_3 \bullet 9H_2O$, Na_2CO_3, K_2CO_3, NaOH, and KOH with various concentrations. The composite activator of $Na_2SiO_3 \bullet 9H_2O$+KOH exerts the highest activation efficiency evidenced by the enhanced strength, proposing the synergy activation between the inherent ≡Si-O-Si≡ chains derived from Na_2SiO_3 and K^+'s catalysis. It reveals that the K^+ plays a crucial role in geopolymerations with the prerequisites of some inherent ≡Si-O-Si≡ chains as the "condensation nucleus", boosting the crosslinking and propagation of N-(C)-A-S-H chains. The as-formed amorphous siliceous sols also could fill into the pores or holes and present a compact morphology, leading to an increase in the pore volume of the diameter less than 100 nm, as well as an increase in weight loss temperatures from TG/DTG results. It explores an efficient and cost-effective preparation of fly ash-based geopolymer for developing solid-waste recycling techniques.

Acknowledgments: This work is supported by the Natural Science Foundation of Shaanxi Province (2022JM-222), Social Science Foundation of Shaanxi Province (2022R046), the open fund from Key Laboratory of Solid Waste Treatment and Resource Recycling, Ministry of Education, Southwest University of Science and Technology (22kfgk02).

References

1. Deventer J, Provis J, Duxson P, et al. Reaction mechanisms in the geopolymeric conversion of inorganic waste to useful products. Journal of Hazardous Materials A,139 (2007) 506–513.
2. Fernández-Jiménez A, Palomo A, Criado M. Microstructure development of alkali-activated fly ash cement: a descriptive model. Cement and Concrete Research, 35 (2005) 1204–1209.
3. Wang S, Liu B, Zhang Q, et al. Application of geopolymers for treatment of industrial solid waste containing heavy metals: State-of-the-art review. Journal of Cleaner Production, 390 (2023) 136053
4. Peng X, Li H, Hu Y. Preparation of metakaolin-fly ash cenosphere based geopolymer matrices for passive fire protection. Journal of Materials Research and Technology, 23 (2023) 604-610.
5. Harmal A, Khouchani O, El-Korchi T, et al. Bioinspired brick-and-mortar geopolymer composites with ultra-high toughness. Cement and Concrete Composites, 137 (2023) 104944.
6. He M, Yang Z, Li N, et al. Strength, microstructure, CO_2 emission and economic analyses of low concentration phosphoric acid-activated fly ash geopolymer. Construction and Building Materials, 374 (2023) 130920.
7. Sarıdemir M, Çelikten S. Effects of Ms modulus, Na concentration and fly ash content on properties of vapour-cured geopolymer mortars exposed to high temperatures. Construction and Building Materials, 363 (2023) 129868.
8. Komljenovic M, Bascarevic Z, Bradic V. Mechanical and microstructural properties of alkali-activated fly ash geopolymers. Journal of Hazardous Materials, 181 (2010) 35–42.
9. Cheng T, Chiu J. Fire-resistant geopolymer produced by granulated blast furnace slag. Minerals Engineering, 16 (2003) 205–210.
10. Tchakouté H, Rüscher C, Kong S, et al. Geopolymer binders from metakaolin using sodium water glass from waste glass and rice husk ash as alternative activators: A comparative study. Construction and Building Materials, 114 (2016) 276–289.
11. Esaifan M, Khoury H, Aldabsheh I, et al. Hydrated lime/potassium carbonate as alkaline activating mixture to produce kaolinitic clay based inorganic polymer. Applied Clay Science, 126 (2016) 278-286.
12. Wang W, Fan C, Wang B, et al. Workability, rheology, and geopolymerization of fly ash geopolymer: Role of alkali content, modulus, and water–binder ratio. Construction and Building Materials, 367 (2023) 130357.
13. Yan S, Pan D, Dan J, et al. Calcium carbide residue and Glauber's salt as composite activators for fly ash-based geopolymer. Cement and Concrete Composites, 140 (2023) 105081.

14. Yang J, Bai H, He X, et al. Performances and microstructure of one-part fly ash geopolymer activated by calcium carbide slag and sodium metasilicate powder. Construction and Building Materials, 367 (2023) 130303.
15. Wang H, Zhao X, Gao H, et al. The effects of salt-loss soda residue and oxalate acid on property and structure of fly ash-based geopolymer. Construction and Building Materials, 366 (2023) 130214.
16. Yliniemi J, Nugteren H, Illikainen M, et al. Lightweight aggregates produced by granulation of peat-wood fly ash with alkali activator. International Journal of Mineral Processing 149 (2016) 42–49.
17. Görhan G, Kürklü G. The influence of the NaOH solution on the properties of the fly ash-based geopolymer mortar cured at different temperatures. Composites: Part B, 58 (2014) 371–377.
18. Somna K, Jaturapitakkul C, Kajitvichyanukul P, et al. NaOH-activated ground fly ash geopolymer cured at ambient temperature. Fuel, 90 (2011) 2118–2124.
19. Chindaprasirt P, Thaiwitcharoen S, Kaewpirom S, et al. Controlling ettringite formation in FBC fly ash geopolymer concrete. Cement & Concrete Composites, 41 (2013) 24–28.
20. Prudhomme E, Michaud P, Joussein E, et al. Role of alkaline cations and water content on geomaterial foams: Monitoring during formation. Journal of Non-Crystalline Solids, 357 (2011) 1270–1278.
21. Guerrieri M, Sanjayan J. Behavior of combined fly ash/slag-based geopolymers when exposed to high temperatures. Fire Material, 34 (2010)163–175.
22. Kürklü G. The effect of high temperature on the design of blast furnace slag and coarse fly ash-based geopolymer mortar. Composites Part B, 92 (2016) 9-18.
23. Vassilev S, Baxter D, Vassileva C. An overview of the behaviour of biomass during combustion: Part I. Phase-mineral transformations of organic and inorganic matter. Fuel, 112 (2013) 391–449.
24. MarieSkofteland B, Ellesad O, Lillerud K. Potassium merlinoite: crystallization, structural and thermal properties. Microporous and Mesoporous Materials 43 (2001) 61-71.
25. Lee W, Deventer J. Structural reorganisation of class F fly ash in alkaline silicate solutions. Colloids and Surfaces A: Physicochem. Eng. Aspects 211 (2002) 49-66.
26. Korina T. Ion exchange in amorphous alkali-activated aluminosilicates: Potassium based geopolymers. Applied Clay Science 87 (2014) 205–211
27. Wang Y, Zhao J. Comparative study on flame retardancy of silica fume-based geopolymer activated by different activators. Journal of Alloys and Compounds, 743 (2018) 108-114.
28. Yang J, Zhang Q, He X, et al. Low-carbon wet-ground fly ash geopolymer activated by single calcium carbide slag. Construction and Building Materials, 353 (2022) 129084.
29. Murri A, Medri V, Ruffini A, et al. Study of the chemical activation of hydroxyapatite rich ashes as raw materials for geopolymers. Ceramics International, 41 (2015) 9734–9744.
30. Peng Z, Vance K, Dakhane A, et al. Microstructural and ^{29}Si MAS NMR spectroscopic evaluations of alkali cationic effects on fly ash activation. Cement & Concrete Composites, 57 (2015) 34–43.
31. Cioffi R, Maffucci L, Santoro L. Optimization of geopolymer synthesis by calcination and polycondensation of a kaolinitic residue. Resources, Conservation and Recycling, 40 (2003) 27–38.
32. Hwang C, Huynh T. Effect of alkali-activator and rice husk ash content on strength development of fly ash and residual rice husk ash-based geopolymers. Construction and Building Materials, 101 (2015) 1–9.